CRITICAL RAW MATERIALS ELIMINATION BY A TOP-DOWN APPROACH TO HYDROGEN AND ELECTRICITY GENERATION

Grant agreement no.: 721065

***Start date**: 01.01.2017 – **Duration**: 42 months*

***Project Coordinator**: CNRS*

DELIVERABLE REPORT

DELIVERABLE 3.1 – CRM-FREE OER AND HER CATALYST TO WP5 FOR AEMEL TESTING	
Due Date	31/10/2017 (M10)
Author(s)	Tanja Kallio, José-Ramón Galan-Mascaros, Frédéric Jaouen, Dario Dekel
Work Package	WP3: Catalyst synthesis and characterization
Work Package Leader	Tanja Kallio (AALTO)
Lead Beneficiary	AALTO
Date released by WP Leader	30/10/2017
Date released by Coordinator	31/10/2017

DISSEMINATION LEVEL		
PU	*Public*	***PU***
PP	*Restricted to other programme participants (including the Commission Services)*	
RE	*Restricted to a group specified by the consortium (including the Commission Services)*	
CO	*Confidential, only for members of the consortium (including the Commission Services)*	

NATURE OF THE DELIVERABLE		
R	*Report*	
P	*Prototype*	
D	*Demonstrator*	***D***
O	*Other*	

SUMMARY	
Keywords	oxygen evolution reaction, hydrogen evolution reaction, alkaline media, electrocatalyst, catalyst, critical raw material
Full Abstract (Confidential)	The report presents activity and stability data for selected electrocatalysts investigated during M1-M10 in CREATE for HER and OER in alkaline medium. For OER, unsupported binary and ternary ZnFe and NiZnFe metal oxides show the highest OER activity (optimized metal ratios). Increased activity is observed after electrochemical cycling for $Ni_{33}Zn_{33}Fe_{33}O_x$, reaching *ca* 50 % of the internal CREATE target of activity and passing the stability criterion. Interfacing this OER active phase with a high surface area conductive Ni support will be explored to further increase the activity. For HER, low Pt content on SWNT and CRM-free N-doped CNT were selected as best representative of CRM-lean and CRM-free alternatives. While the low Pt/SWNT approach reaches both the internal activity and stability targets, the N-CNT approach results in stable but too little active materials. CRM-free but metal-based HER catalysts will be investigated in the near future to close the activity gap for CRM-free HER catalysts.
Publishable Abstract (If different from above)	

REVISIONS			
Version	**Date**	**Changed by**	**Comments**
1.0	13.10.2017	Tanja Kallio (AALTO)	
1.1	16.10.2017	Frédéric Jaouen (CNRS)	
1.2	26.10.2017	JR Ramón Galán (ICIQ)	
1.3	26.10.2017	Taneli Rajala (AALTO)	
2.1	27.10.2017	Tanja Kallio (AALTO)	
3.0	31.10.2017	Frédéric Jaouen (CNRS)	

Set of CRM-FREE OER AND HER CATALYST WITH ACTIVITY VERIFIED BY RDE SENT TO WP5 FOR AEMEL TESTING

CONTENTS

INTRODUCTION

The purpose of D3.1 is to demonstrate the preparation of a first set of CRM-free and low-CRM catalysts developped in CREATE and with significant activity and stability toward the electrode reactions occurring in an alkaline electrolyzer, with activity and stability verified in rotating disk electrodes.

In an electrolyser, two electrochemical reactions occur, namely the hydrogen evolution reaction (HER) on the cathode and the oxygen evolution reaction (OER) on the anode. A first set of catalysts for both reactions are demonstrated in the present deliverable, and those catalysts have been transferred to WP5 in sufficient amount for subsequent testing in AEMEL devices with reference commercial AEM membrane from FUMATECH.

Although the ultimate focus of the CREATE project is on the development, for AEMEL devices, of critical raw material (CRM) free catalysts (the list of CRMs as defined by the EU can be accessed at http://eur-lex.europa.eu/legal-content/EN/ALL/?uri=COM:2017:0490:FIN, both CRM-free and CRM-lean alternatives are considered in this deliverable for catalyzing the HER in alkaline medium, as a trade-off between cost and performance. This is necessary as the targeted activity performance for the HER in alkaline medium is not yet achieved with composite catalysts that are entirely free of CRM.

Test protocols for the electrochemical activity and durability measurements as well as pass/fail criteria for catalyst intended for each reaction were defined in WP2 (Technical Specifications, Cost Analysis & Life Cycle) of CREATE, and reported in Deliverable 2.1. In the following, the material performance is reflected against these criteria as well as relative to recognized state-of-the-art electrocatalysts for the HER and OER in alkaline electrolyte.

1. OER CATALYST

1.1 EXPERIMENTAL CONDITIONS AND PROTOCOL FOR OER ACTIVITY MEASUREMENT

The electrochemical experiments were performed with a Biologic SP-150 potentiostat. Ohmic drop was compensated using the positive feedback compensation implemented in the instrument. All experiments were performed with a three-electrode configuration using 0.1 M KOH (pH 13) as electrolyte solution, employing a graphite rod as counter electrode, a Hg/HgO (NaOH 1 M) reference electrode and catalyst-ink deposited on nickel support as working electrode. The catalyst-ink was prepared in 1 mL of ethanol: water (3:1), containing 10 mg catalyst and 10 wt. % ionomer (FAA-3 ionomer from Fumatech, at 5 wt. %). Then 6 µL of ink were drop-casted on the clean surface of a nickel Rotating Disk Electrode (Ni-RDE) and dried at 60°C to obtain a total loading of 840 µg catalyst·cm^{-2}. Before the electrochemical activity measurement, a drop of water is deposited on the electrode, the tip screwed on the rotating shaft and the shaft slowly immersed in electrolyte, to minimize entrapment of air bubbles during immersion. N_2 was then bubbled in the solution for 10 min. Then, a current interrupt (CI) of 0.5 mA was applied with a frequency of 0.2 s (10 times) to estimate the iR-drop. Afterwards, a polarization curve is cycled at 75 mV·s^{-1} between 1.0 and 1.5 V *vs*. RHE for 10 cycles (break-in procedure). The polarization measurements from which OER activity is extracted were recorded at 1 mV·s^{-1} in the same potential range.

1.2 EXPERIMENTAL CONDITIONS AND PROTOCOL FOR OER STABILITY MEASUREMENT

Accelerated stability tests (AST) were performed by comparison between the initial polarization curve (following the procedure described above) and the polarization curve obtained with the same electrode after 5000 cycles between 1.3 and 1.7 V *vs*. RHE at 100 mV·s^{-1} at rotation rate of 800 rpm (AST protocol Nr 7 in D2.1).

1.3 SYNTHESIS OF OER CATALYSTS

All reagents were commercially available and used as received. Mixed metal oxides were prepared by modified literature methods [1,2,3]. Metal nitrates, in the appropriate ratio, were dissolved in 50 mL of distilled water with constant stirring until a clear solution was obtained. The iron concentration was fixed to 0.0125 M and, then, the corresponding amount of each metallic precursor was calculated according to the desired composition. Glycine was added into the aqueous solution (glycine/metal molar ratio = 1.20) and stirred until total dissolution. Afterwards, the solution was heated up to 200^{o}C until total solvent evaporation and glycine combustion. The resulting porous dark solid was recovered and calcined at 1100^{o}C in a tubular oven for 1 hour. Finally, calcined material was mechanically milled in an Agate ball milling jar (2 Agate balls) at 1500 rpm for 15 minutes. In general, for all oxides the yield per batch is ≈ 100 mg.

1.4 ACTIVITY OF OER CATALYSTS

The polarization curves for the best OER catalysts prepared in CREATE thus far are shown in Fig. 1, that correspond to $NiZnFeO_x$ (NiZnFe_33:33:33); $ZnFe_9O_x$ (ZnFe_10:90); $ZnFe_2O_x$ (ZnFe_33:66); and Fe_2O_3. We used Ni-Raney as a Fe-free and Zn-free blank, for comparison.

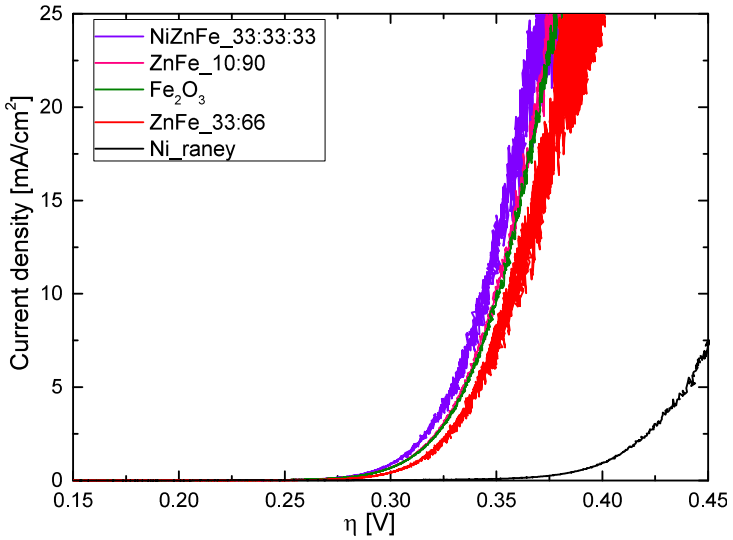

Fig.1 Initial OER polarization curves for the best metal-oxides, measured immediately after break-in. Scan rate 1 mV·s^{-1}, 0.1 M KOH, room temperature, catalyst loading 840 µg cm^{-2} on Ni-RDE support, ionomer binder FAA-3.

The Tafel representation of the polarization curves (Fig. 2) shows that the ZnFe binary oxide (ZnFe 33:66 and ZnFe 10:90) and the NiZnFe ternary oxide (NiZnFe 33:33:33) have lower onset-potentials and lower Tafel slopes than the corresponding NiFeOx and NiCrFeOx binary and ternary oxide compounds, that were already reported [4]. We associate these lower values (higher activity) with the presence of Zn in the spinel phase, changing the structural properties and modifying the transport mechanism. Additionally, α-Fe_2O_3 (hematite) exhibits very good electrocatalytic performance, in contrast with the available reports on this iron oxide.

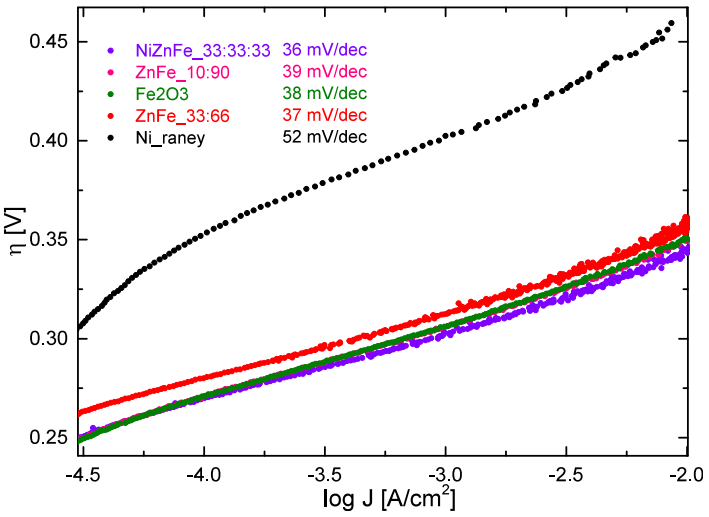

Fig.2 Tafel representation of the initial OER polarisation curves, extracted from the data shown in Fig. 1.

ELECTROCHEMICAL STABILITY OF OER CATALYSTS

The results of the electrochemical AST protocol for OER that was described in 1.2 are shown in Fig. 3. Surprisingly, $NiZnFeO_x$ shows improved OER activity after the AST protocol designed for OER catalysts. Although to a lower extent, increased activity following AST is also observed for $NiFe_2O_x$. These are the two pure spinel phases. In contrast, $ZnFe_9O_x$ and hematite show higher overpotentials of 7 and 16 mV, respectively after the AST. The current densities achieved at 320 mV overpotential are summarized in Table 1.

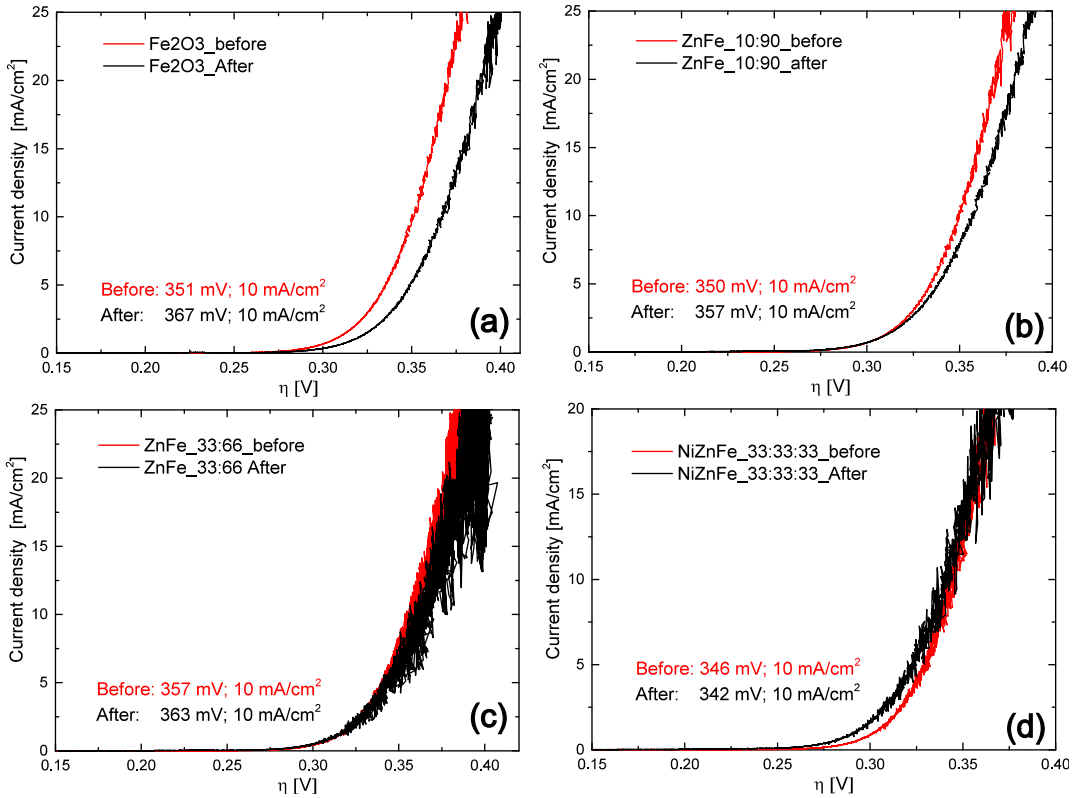

Fig.3. Stability of OER catalysts. Polarization curves before (red curve) and after (black curve) 5000 cycles. The numbers in the figure indicate the overpotential required to reach 10 mA·cm^{-2}. The internal CREATE pass/fail value for transfer to AEMEL is 320 mV (1.55 V vs. RHE).

Table 1. Current density values reported at fixed overpotential for various metal-oxides before and after the AST.

Metal-Oxide Catalyst	Initial current density @ η = 320 mV (1.55 V *vs.* RHE) / mA·cm^{-2}	Final current density @ η = 320 mV (1.55 V *vs.* RHE) / mA·cm^{-2}
Fe_2O_3	2.22	1.18
ZnFe_33:66	1.50	1.86
ZnFe_10:90	2.27	2.13
NiZnFe_33:33:33	3.06	4.80

1.7 COMPARISON TO STATE-OF-THE-ART AND TO INTERNAL CREATE TARGETS

We identified the most active OER electrocatalysts in alkaline medium as those reported by Boettcher *et al*. and Stahl.[1,4] According to our protocols, the four catalysts we describe in this report are superior to the most active catalysts reported in those reports. However, the scalars they report are higher than the ones we internally measured for very similar materials (same crystallographic structure and elemental ratios). Boettcher's most active OER catalyst, Ni_9FeOx, reaches 10 $mA{\cdot}cm^{-2}$ of current density at an overpotential of 336 mV with a Tafel slope of 30 mV/dec. However, those data were obtained at pH 14, and in the absence of a polymer binder. The oxides were self-standing, as prepared on the electrode support. Stahl's most active OER catalyst, identified via combinatorial screening of nearly 3500 trimetallic $A_xB_yC_zO_q$ mixed metal-oxide compositions were Ni-Fe-Al (40:40:20), Ni-Fe-Cr (40:20:40) and Ni-Fe-Ga (20:20:60). These OER catalysts reach 6.3, 5.6 and 25.0 $mA{\cdot}cm^{-2}$, respectively, at 345 mV overpotential, at pH 13. Cr and Ga however belong to the list of CRMs as defined by the EU (see cited document in the introduction). Regarding spinel-type OER catalysts, our materials are superior to structurally analogous oxides reported as catalysts for water oxidation [4, 5–7]. Some Ni ferrites were reported for oxygen production, showing onset overpotentials around 380 mV and Tafel slope about 60 mV/dec [8]. This performance was slightly improved via morphology control or additional doping [5,9]. It is important to mention that all these catalysts were characterized as single phases, being directly deposited on electrode supports. In our case, we systematically used an ionomer binder.

In this context, our main achievement has been the identification of Zn as a promising component of these oxides. Maybe due to the poor redox activity, Zn has not been investigated in previous studies. The presence of Zn^{2+} cations clearly improves the electrocatalytic performance, according to our data. We assign this observation to two main factors. On one hand, the presence of Zn^{2+} in the spinel structure has positive effects in the electron transfer conductivity of the material. It has been reported that Zn doping increases electrical conductivity of Fe_2O_3 and $NiFe_2O_4$ due to the formation of $ZnFe_2O_4$ and $Ni_{1-x}Zn_xFe_2O_4$ spinel phases. Ni^{2+} ions strongly prefer the occupation of octahedral sites, whereas Zn^{2+} prefers to occupy tetrahedral ones. Therefore, Fe ions which exist in Fe^{2+} and Fe^{3+} states, occupy both tetrahedral and octahedral sites. As Zn substitution increases, replacing Ni ions, some Fe ions are forced to migrate from tetrahedral to octahedral positions. As a result, the number of Fe^{2+} and Fe^{3+} ions increase at octahedral positions, facilitating the hopping between Fe^{3+} and Fe^{2+} sites, and increasing the electric conductivity of the spinel material [1,10]. We cannot discard a second possible positive effect. During operation or electrochemical cycling, some Zn will leach from the material, possibly increasing the total active area of the catalyst. This leaching should correspond only to surface Zn positions, and should stop once all surface available Zn sites are removed. Stability tests indicate that the Zn-containing materials have stable OER activity in the long term, and their activity can even improve after multiple runs.

Finally, we also compared our results with $NiFeO_x$ supported on Raney Ni, provided by Prof. Mukerjee (Northeastern Univ. Boston, USA). This supported $NiFeO_x$ catalyst shows overall better performance than our unsupported oxides. Therefore, we expect that a combination of our most active catalyst with a Raney Ni support (nanoparticles, or large surface area electrodes) should allow us reaching the target performance parameters. However, the AST for $NiFeO_x$ on Raney Ni was not fully satisfactory (Fig. 4). The apparent OER activity improves after cycling, but the appearance of a new pre-catalytic event at 200-220 mV overpotential indicates that the original catalyst is actually evolving during electrochemical cycling. This, questions the stability of this material (massive leaching during AST?) and the nature of the active surface after AST. Indeed, the apparent higher activity of $NiFeO_x$ on Raney Ni after AST may be related to the appearance of this irreversible pre-catalytic event. Longer stability tests will be performed as well as intermediate OER-activity measurements between cycle 1 and cycle 5000, to investigate whether the increase in OER activity is related to the pre-peak event. This will also be coupled to online detection of metal leaching, and also post-AST determination of metal content leached in the electrolyte.

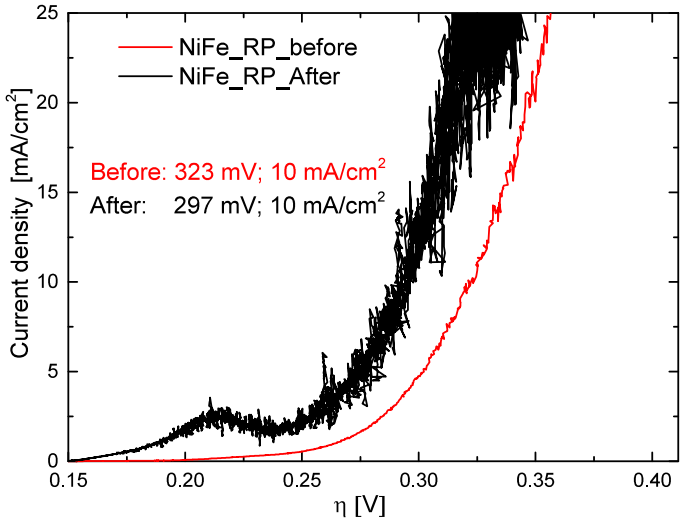

Fig.4. Stability of OER catalysts. Polarization curves before (red curve) and after (black curve) 5000 cycles.

2. HER CATALYST

2.1 EXPERIMENTAL CONDITIONS AND PROTOCOL FOR HER ACTIVITY MEASUREMENT

Rotating disk electrode (RDE) experiments for HER catalysts were performed in 0.1 M KOH at 25 °C, using IrO_2 as the counter electrode and RHE as the reference. Catalyst was deposited on a glassy carbon disk of 5 mm diameter, constituting the working electrode. Ink for the deposition was prepared by carefully dispersing catalyst powder in solvent so that pipetting the ink on the working electrode results in catalyst loading of 200 µg·cm^{-2} followed by addition of 5 µl of diluted Nafion ionomer solution (50 µl of 5 wt-% Nafion in 2 ml of ethanol).

Before measuring the activity, a break-in procedure was implemented. The dried catalyst layer on the glassy carbon was first contacted with d-water, either by dropping hot deionized-water on top or by immersing the catalyzed RDE tip in a vial with hot milli-Q water (50-60 °C). The RDE was then screwed on the rotating shaft and immersed in the electrolyte. Nitrogen was bubbled in the electrolyte for 15-30 min, after which it was directed above the electrolyte, cycling the potential between −0.4 to 0.0 V *vs.* RHE at 50-100 mV·s^{-1} until CVs were reproducible.

For the activity measurement, the electrolyte was saturated with H_2 for about 30 min until OCP stabilized. Polarization curves were measured at 1-2 mV·s^{-1} starting from OCP to −0.4 V *vs*. RHE and back to 0.0 V *vs*. RHE (only one cycle if positive and negative going scans superimposed, two or more otherwise) at 2500 rpm rotation to help removing hydrogen evolved at the surface of the working electrode. During this polarisation, the counter electrode is at OCP or performs the OER, which should not lead to leaching of Ir.

2.2 EXPERIMENTAL CONDITIONS AND PROTOCOL FOR HER STABILITY MEASUREMENT

The stability of the catalyst material was evaluated using an accelerated stress tests (AST) defined in ere defined in WP2 (Technical Specifications, Cost Analysis & Life Cycle) of CREATE, and reported in Deliverable 2.1. For the present HER materials for alkaline medium, AST Nr. 9 was applied, and is depicted below. The electrode rotation was kept at 2500 rpm during the 5000 cycles. The catalyst passes the stability test if the potential shift due to the cycling was no more than 80 mV at a given current density.

Table 2. Definition of the AST for HER catalysts (AST 9).

	Electrolyte	Signal shape	Number of cycles	lower / upper potential limits	Scan rate (LSV) or dwell time (Stairs)
AST 9	N_2-satd 0.1 M KOH	LSV	5 000	-0.4 – 0.0 V vs RHE	100 mV s^{-1}

2.3 Synthesis of HER catalysts

2.3.1. Synthesis of CRM-free N-CNT

Nitrogen-doped carbon nanotubes can be synthesized using number of different approaches. Here two post-synthesis doping methods were investigated. In a first approach [11], CNTs are first treated with strong acid to induce functional groups and this is followed by the synthesis of polyaniline in the presence of the acid-treated CNTs. The final step is a heat-treatment procedure at T > 700°C under inert atmosphere. In the other method [12], CNTs and emeraldine salt are first dispersed in two separate mild acid solutions and these dispersions are subsequently combined and the mixing is continued. After separation of the CNT composite, it is subjected to a heat treatment similar to the one described above.

2.3.2 Synthesis of Pt/SWNT with ultralow CRM content

HER catalysts with an ultralow amount of Pt on single-wall carbon nanotubes (SWNTs) were prepared by atomic layer deposition (ALD). The pulse lengths of the Pt and oxidizer precursors were varied, which expectedly resulted in improved electrochemical activity for longer pulses. In comparison, Pt/SWNT was also prepared via a simple suspension synthesis where SWNTs and Pt precursor were carefully mixed with a solvent. After post-treatment, this resulted in Pt/SWNTs showing comparable performance to the ALD approach.

Fig. 5 displays the size and distribution of Pt particles on the SWNTs produced by the above-mentioned methods. Mass percentages will be analysed with ICP-MS by Jülich FZ in December.

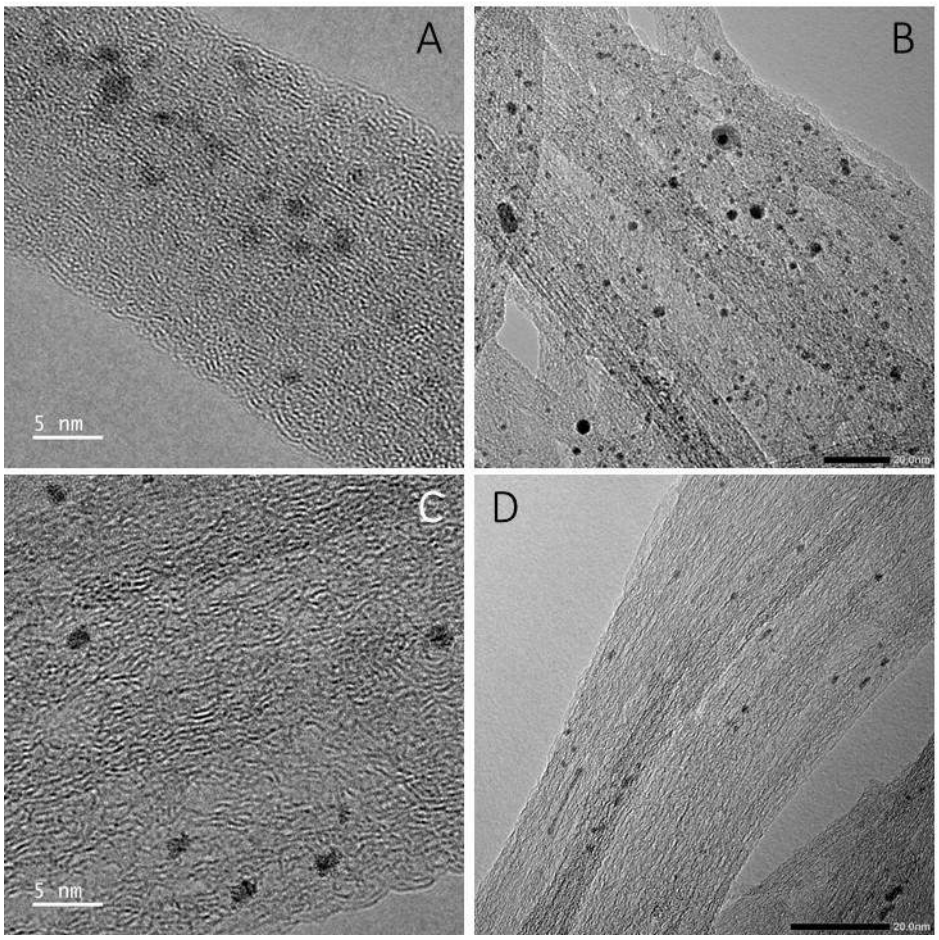

Fig. 5. TEM images of the prepared Pt/SWNT catalysts. A and B refer to the ALD method (ALD-1); C and D to the suspension synthesis. Scale bar is 5 nm on the left and 20 nm on the right

2.4 Electrochemical Activity of HER Catalysts

Fig. 6 represents an example of obtained HER activities for the catalysts prepared by ALD and suspension synthesis (ss) in comparison with N-CNT and pristine SWNT. The enhancing effect of Pt is clearly seen in higher current densities throughout the entire potential window and also in the lower onset potential (0 V) with respect to the N-CNT (−140 mV onset potential). When comparing the ALD catalysts with each other, the one having longer pulse time (ALD-1) performs better at high overpotential.

We associate the enhanced activity trend in Fig. 7 with higher loading and better distribution of Pt particles. Improved performance of the ALD catalyst with respect to the suspension synthesis is in accordance with the TEM images seen in Fig. 5, where ALD-1 material (subfigures A and B) appears to have more densely distributed catalyst particles on the SWNT surface than the one from suspension synthesis (subfigures C and D).

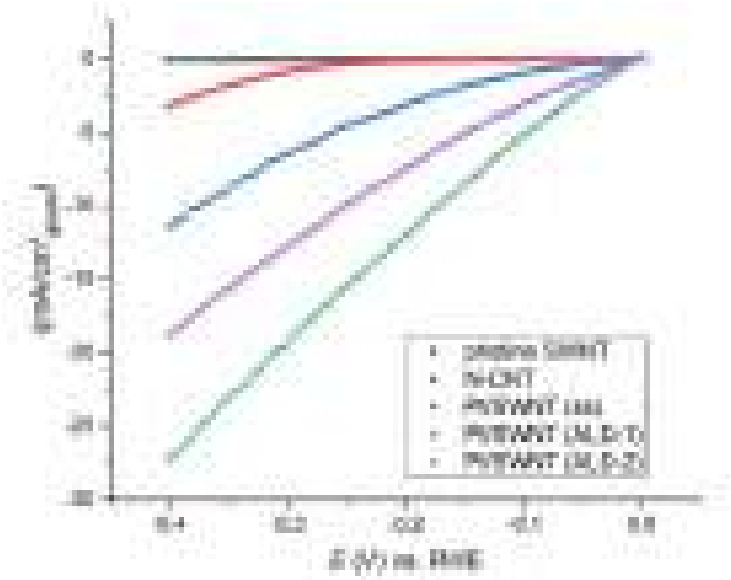

Fig. 6. Initial HER polarization curves for the synthesized Pt/SWNT catalysts and for N-CNT and pristine SWNT. Data measured in H_2 saturated 0.1 M KOH. Scan rate 2 mV·s^{-1}, rotation rate 2500 rpm. Total catalyst loading 200 µg cm^{-2} (C, N and metal contents).

Tafel slopes (Fig. 7) generated from Fig. 6 show expectedly that all the Pt-containing catalysts have lower onset potentials and Tafel slopes than N-CNT.

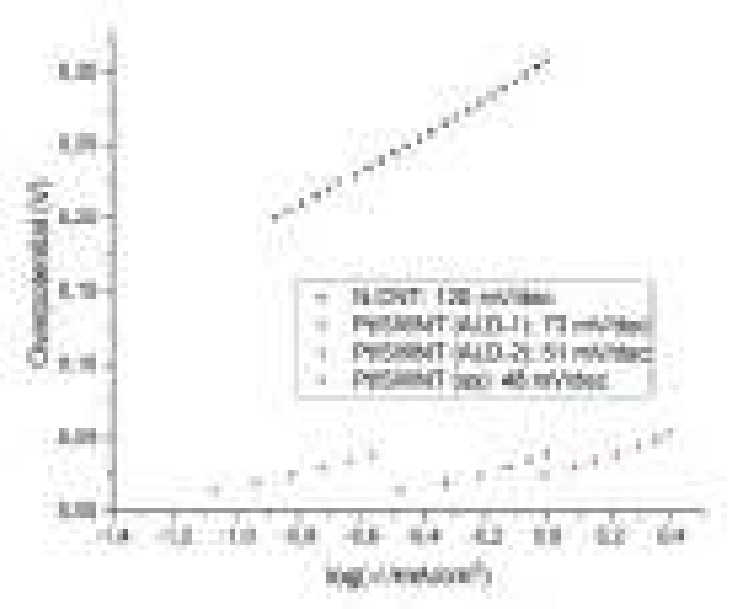

Fig. 7. Tafel representation of the polarization data of Fig. 6.

2.5 Electrochemical stability of HER catalysts

The stability test result for Pt/SWNT (ALD-1) is shown in Fig. 8. At the highest current density of 26.5 mA/cm^2, the difference in potential is only 10 mV.

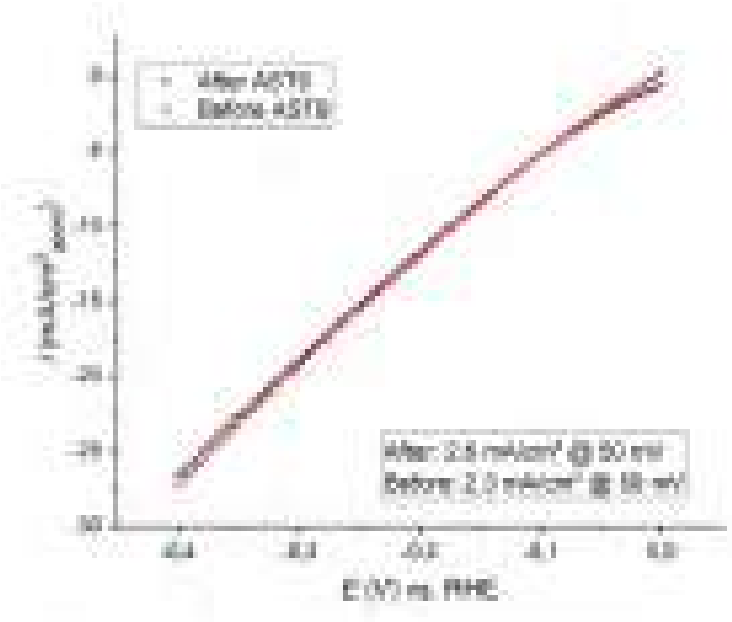

Fig. 8. HER polarization curves for Pt/SWNT (ALD-1) before and after the stability test (AST 9) in 0.1 M KOH, scan rate 2 mV/s, rotation rate 2500 rpm.

2.6 Comparison to state-of-the-art and to internal CREATE targets

Kinetic current densities at –0.05 V *vs*. RHE were 0.02, 0.4, 2.3 mA·cm^{-2} and 1.3 mA·cm^{-2} for N-CNT, Pt/SWNT(ss), Pt/SWNT(ALD-1) and Pt/SWNT(ALD-2), respectively. In other words, at this moment, only Pt/SWNT(ALD-1) passes the HER activity criterion defined for HER catalysts in CREATE Deliverable 2.1.

Table 3. HER overpotentials @ 10 mA/cm2 in 1 M KOH at 25 °C.

Catalyst	**–η (mV)**	**Ref.**
Ni/rGO	231	[13]
Co,N-doped CNT	240	[14]
Mo_2C-NCNT	257	[15]
Ni_3S_2/MWCNT-NC	340	[16]
Fe_2P/NGr	355	[17]

Fig. 8 shows that our material Pt/SWNT (ALD-1) passes also the HER stability criterion defined in Deliverable 2.1 (maximum acceptable change in overpotential of 80 mV after AST 9).

Pt/SWNT(ALD-1) shows comparable kinetic activity to Pt/C by Sheng *et al*. [18] but only a very rough comparison is sensible, before finishing ICP-MS analysis. While platinum is still the benchmark for

metallic HER catalysts, promising alternatives are being investigated from the first-row of transition metals, among which Ni-composites are considered state-of-the-art. Wang *et al*. have recently synthesized Ni/g-C_3N_4 catalyst that outperforms other Ni-based materials and comes close to commercial Pt/C catalyst [19]. In 0.1 M KOH, Huang *et al*. report 10 mA/cm^2 @ 300 mV for Ni-graphene [20]. Table 3 summarizes transition-metal-based results in 1 M KOH from other groups. As for carbon-based and metal-free materials, Qu et al. report electrochemical activity for HER in alkaline for their dual-doped N,S-CNT, obtaining 5 mA/cm^2 @ 400 mV overpotential [21].

In addition to the above described investigation of CRM-free and CRM-lean HER catalysts, screening of CRM-free transition metal based alternatives is on-going. In CREATE, we are currently screening several bimetallic Ni-based materials with combinatorial tools, in order to identify active and stable HER electrocatalysts. After identifying promising alternatives, nanoparticle catalyst will be synthetized and their activity and stability measured using the protocols described in Deliverable 2.1 and used here for HER evaluation. Furthermore, Ni based nitrides and sulphides will also be evaluated in the near future.

REFERENCES

[1] Trotochaud, L., Ranney, J. K., Williams, K. N. & Boettcher, S. W. *J. Am. Chem. Soc*., 134, 17253 (2012).
[2] Costa, A. C. F. M., Tortella, E., Morelli, M. R., Kaufman, M. & Kiminami, R. H. G. A., *J. Mater. Sci.,* 37, 3569 (2002).
[3] Islam, M. U. *et al*. *Solid State Commun*., 130, 353 (2004).
[4] Gerken, J. B., Shaner, S. E., Masse, R. C., Porubsky, N. J. & Stahl, S. S., *Energy Environ. Sci*., 7, 2376 (2014).
[5] Liu G., Gao X., Wang K., He D., Li J., *Int. J. Hydrogen Energy*, 41, 17976 (2016).
[6] Liu G., Wang G., Gao X., He D., Li J., *Electrochim. Acta*, 211, 871 (2016).
[7] Díez-García M., Lana-Villarreal T., Gómez R., *ChemSusChem*, 9, 1504 (2016).
[8] Su Y-Z, *et al., Electrochim.a Acta*, 174, 1216 (2015).
[9] Cady C., *et al., ACS Catalysis* 5, 3403 (2015).
[10] Umapathy, G., Senguttuvan, G., Berchmans, L. J. & Sivakumar, V., *J. Mater. Sci. Mater. Electron*., 27, 7062 (2016).
[11] Nikolic, M. V. *et al*., *Sci. Sinter*., 44, 307 (2012).
[12] Borghei, M., *et al*., Appl. Catal. B: Environ. 158–159, 233 (2014).
[13] F. Davodi et al., *J. Catal* 353,19 (2017) 19.
[14] Zhiani, M., et al., Electrocatalysis 7.6,466 (2016)
[15] Gao, S., *et al*., *Nanoscale* 7.6, 2306 (2015).
[16] Zhang, Kai, et al., *J. Mater. Chem. A* 3.11, 5783 (2015).
[17] Lin, T.-W., *et al*., *Appl. Catal. B: Environ*. 154,213 (2014).
[18] Huang, Z., *et al*., *Nano Energy* 12,666 (2015).
[19] Sheng, W., et al., *J Electrochem Soc* 157.1, B1529 (2010).
[20] Wang, L., *et al*., *ACS Sustain. Chem. Eng*. 5.9, 7993 (2017).
[21] Huang, Y., et al., Int. J. Hydrog. Energy 41.6, 3786 (2016).
[22] Qu, K., *et al*., Adv. *Energy Mater.* 7.9 (2017).